CP4O

CryoSat Plus for Oceans

ESA/ESRIN Contract No. 4000106169/12/I-NB

D4.1 – Algorithm Theoretical Basis Document on the Improved Wet Tropospheric Correction for CryoSat-2

VERSION 1.0, 11 June 2014

Author(s)	**Affiliation**
M. Joana Fernandes	U.Porto & CIMAR-LA/CIIMAR-UP
Clara Lázaro	U.Porto & CIMAR-LA/CIIMAR-UP
Alexandra L. Nunes	IPP/ISEP & CIMAR-LA/CIIMAR-UP

Contents

1. Introduction

With an absolute value up to 50 cm and highly variable in space and time, the path delay due to the presence of water vapour in the atmosphere, or wet tropospheric correction (WTC), is still one of the major error sources in satellite radar altimetry. Due to its high variability, the most accurate way to model this effect over open-ocean is through the measurements of microwave radiometers (MWR) on board the altimetric missions. In spite of the continuous progress in the modelling of this effect by means of numerical weather models (NWM) (e.g., Miller et al., 2010; Dee et al., 2011), the accuracy of present NWM-derived WTC is still not good enough for most altimetry applications such as sea level variation. Indeed, an accurate enough modelling of this effect can only be achieved through actual measurements of the atmospheric water vapour content at the time and location of the altimetric measurements. For this purpose, dedicated near-nadir looking, single measurement microwave radiometers (RA-MWR) have been incorporated in the most recent altimetric missions.

CryoSat-2 (CS-2), primarily dedicated to measuring and monitoring the changing thickness of ice in polar regions, does not carry an on-board RA-MWR. Instead a model-based wet tropospheric correction is applied to CS-2 data, provided by the European Centre for Medium-Range Weather Forecasts (ECMWF). The more stringent accuracy requirements imposed by global-scale ocean and coastal studies, however, drove a need to develop an improved correction for CS-2, particularly important for these applications.

The development of a data combination algorithm (DComb) for the computation of an improved WTC, when compared to the one provided by ECMWF, was among the objectives of the ESA-STSE promoted project CP4O – CryoSat Plus for Oceans (ESA/ESRIN Contract No. 4000106169/12/I-NB), a task under the responsibility of University of Porto (U.Porto), as described in CP4O D2.1 – Preliminary Analysis Report. The selected method, designated Data Combination (DComb) algorithm, is based on the approaches followed by Fernandes et al. (2010), Stum et al. (2011) and Fernandes et al. (2013b).

The DComb algorithm estimates the WTC using objective analysis of several available data sources: scanning imaging MWR (SI-MWR) on board remote sensing (RS) satellites, Global Navigation Satellite Systems (GNSS) and the ECMWF Operational Model.

This document presents the data combination algorithm (DComb) developed by U.Porto for the computation of the wet tropospheric correction of CS-2 data over ocean.

2. Overview

The DComb algorithm, develop by U.Porto for the estimation of the WTC for CS-2, estimates the WTC using objective analysis (OA) of several available data sources: scanning imaging MWR (SI-MWR) on board remote sensing satellites, wet path delays derived from GNSS and the ECMWF Operational Model, the best available model for the period of CS-2 mission. A different white noise associated to each data type was adopted. A maximum number of 25 GNSS and 25 SI-MWR measurements were used, those with the largest statistical weights, according to their distance and time difference with respect to the CS-2 measurement for which the correction is being estimated; following the same underlying principle, the closest four ECMWF model grid nodes were also used.

The DComb OA method updates a first-guess value known *a priori* at each location and epoch, in this study the average of the selected GNSS, SI-MWR and ECMWF-derived WTC observations, and provides a quantification of the mapping error associated with each estimated WTC value. The space correlation scales were determined in this study from a set of ECMWF operational model grids at 0.125°×0.125°, well distributed over the year 2013. The resulting spatial correlation scales are within 40 to 93 km. For the temporal correlation scales, a value of 100 minutes was adopted. The WTC signal variance was determined from a 2-years dataset of the ECMWF operational model. The DComb WTC has been computed only for ocean points.

The DComb algorithm was implemented globally and applied both to Jason-2 (J2) and CS-2 for the period from January 2012 to January 2013. Results for J2 allow the comparison of the DComb correction to that from its onboard microwave radiometer, AMR (Advanced Microwave Radiometer). Data from the Radar Altimeter Database System (RADS) were used in this study and its results are presented in D4.2 – Product Validation Report. In addition, the DComb correction was also computed for the months of July 2012 and January 2013 for data files provided by ESA. This latter dataset, which unlike that retrieved from RADS, contains data for all modes of acquisition, was provided as an output for use in the independent validation task performed in WP5000, which will be separately reported in D5.1 – Impact Assessment Report.

The results show that for periods of good data coverage the results are remarkable and the overall improvement with respect to ECMWF operational model is evident.

3. Algorithm Description

3.1 Theoretical Description

3.1.1 Physics of the problem

The total column water vapour (TCWV), also referred to as precipitable water (PW) or integrated water vapour (IWV), is the total water vapour contained in an air column from the Earth's surface to the top of the atmosphere and is usually expressed in kg/m^2 or millimetres (mm), as the length of an equivalent column of liquid water.

The TCWV (abbreviated to *WV* in the following equations) in millimetres is given by

$$WV = \int_0^H \rho_w dz \tag{1}$$

where ρ_w is the water vapour density in kilograms per cubic metre, *z* is the altitude (in m), and *H* is the altitude above which the water vapour density is considered to be negligible.

The path delay due to the water vapour in the atmosphere, the *WTC*, can be estimated from TCWV and atmospheric temperature *T* by (e.g. Keihm et al., 1995):

$$WTC = 1.763 \int_0^H \frac{\rho_w}{T} dz \tag{2}$$

where *WTC* is in metres and *T* is in kelvin.

For practical computations it is most appropriate to replace the vertical integration expressed in Equation (2) by expressions which make use of single level quantities as provided by Numerical Weather Models (NWM) or measured quantities as provided by most measurement systems.

According to Bevis et al., 1994, and as already detailed in D2.1 and in Fernandes et al. (2013b), the *WTC* can be estimated from the total column water vapour, again abbreviated to *WV* in equations, and atmospheric temperature using the following expression:

$$WTC = -\left(0.101995 + \frac{1725.55}{T_m}\right)\frac{WV}{1000} \tag{3}$$

where T_m is the mean temperature of the troposphere, which may be in turn modelled from the surface temperature (T_0) according to, e.g., Mendes (1999), Mendes et al. (2000):

$$T_m = 50.440 + 0.789\, T_0 \tag{4}$$

In Equation (3) and Equation (4), T_0 and T_m are in kelvin, *WV* in millimetres and the *WTC* results in meters.

Alternatively, the dependence of the *WTC* on the atmospheric temperature can be implicitly accounted for by establishing a direct relationship between *WTC* and TCWV (e.g. Keihm et al. (1995), Keihm et al. (2000), Stum et al. (2011), since the ratio between *WTC* and TCWV can be described by a decreasing function of water vapour content, which partly expresses the *WTC* temperature dependence. For example, in Stum et al. (2011), the following relationship was deduced from temperature and humidity profiles from ECMWF model fields:

$$WTC = -(a_0 + a_1 WV + a_2 WV^2 + a_3 WV^3)\, WV \,.\, 10^{-2} \tag{5}$$

with a_0=6.8544, a_1=−0.4377, a_2=0.0714, a_3=−0.0038, *WV* is in cm and *WTC* results in metres.

All space-borne microwave radiometers, both the scanning imaging on board remote sensing satellites (SI-MWR) and the near-nadir looking on board radar altimeters (RA-MWR) make measurements in various water vapor absorption bands of the microwave spectrum. The algorithms for retrieving the TCWV over the ocean from MWR observations are commonly based on a model using the brightness temperatures from channels operating at frequencies ~19, ~22, and 37 GHz; however, when using data from sensors such as AMSU-A or RA-MWR on board ERS, Envisat and SARAL, only observations from two channels are used.

Within WP4000, both approaches, using Equation (3) and Equation (5), were in a first stage considered in order to identify the most suitable for use in the WTC retrieval from SI-MWR water vapour products. Details of the analysis leading to the choice of Equation (3) can be found in Fernandes et al. (2013b). In summary, Equation (5) leads to slightly better results for SI-MWR products previously calibrated with respect to a common reference such as the Advanced Microwave Radiometer (AMR) operated on J2. However, Equation (2) provides equivalent results with the same products but evidences slightly smaller scaling factors with respect to the original products. Therefore, if mixed products are used (previously calibrated and original products) the second approach is preferred.

As far as the estimation of *WTC* from GNSS data are concerned, a detailed description can be found in Fernandes et al., 2010, and Fernandes et al., 2013a.

ECMWF-model-derived *WTC* values have been computed from two single-level parameter fields of the ECMWF operational model at a regular 0.125°×0.125° grid spacing and 6 h intervals, using Equation (3): TCWV and surface temperature (2-m temperature, T_0). Equation (3) gives the *WTC* at the height of the ECMWF model orography. The grid nodes considered in the computations were: all ocean points and land points with altitudes up to 800 m and at distances from coast less than 100 km. For these land points, a height reduction has been applied using the expression by Kouba (2008):

$$WTC(h_0) = WTC(h_s) e^{\frac{h_s}{2000}} \tag{6}$$

In Fernandes et al., 2014, the height dependence of the *WTC* is discussed in the context of altimeter inland water applications. Due to the high variability of the *WTC*, its height dependence is difficult to model and, according to Kouba (2008), this empirical expression should only be used with heights up to 1000 m.

3.1.2 Mathematical description of the algorithm

The methodology for computing the wet tropospheric correction for CryoSat-2 altimeter data that has been implemented, DComb, is based on a data combination of three different datasets by linear space–time objective analysis (OA) technique (Bretherton et al., 1976). The statistical technique optimally interpolates the available wet path delay measurements at each altimeter ground-track point from the nearby (in space and time) SI-MWR, GNSS and ECMWF independent data points. The underlying method, previously developed for coastal altimetry and described in Fernandes et al. (2010), updates a first-guess value known *a priori* at each location and epoch and provides a quantification of the mapping error associated with each estimated WTC value. Only a simplified description of the method is given here. Full details can be found in Bretherton et al. (1976).

The estimate of the WTC field at each point P, F(P), is given by a "first guess", FG(P), plus a weighted average of the set of N *WTC* anomalies X_i^{ano} with respect to the first guess (Equation (8)), at the N points X_i within given space and time search radius around point P:

$$\mathrm{F(P)} = \mathrm{FG(P)} + \sum_{\mathrm{i=1}}^{\mathrm{N}} W_i \ \mathrm{X}_i^{ano} \tag{7}$$

$$\mathrm{X}_i^{ano} = X_i - \mathrm{FG(P)} \tag{8}$$

The weights W_i are estimated from the statistical properties of the *WTC* field:

$$W_i = \sum_{\mathrm{k=1}}^{\mathrm{N}} C_k \ \mathrm{A}_{ik}^{-1} \tag{9}$$

where C_k is the covariance between the computation point P and the nearby measurement point K and is A_{ik}^{-1} is the inverse of the variance–covariance matrix of the *WTC* measurements. Each covariance is normalized by dividing by the variance of the *WTC* field at the estimation point P, so in fact correlations instead of covariances are used.

In practice, the covariance between each pair of points separated by a distance r and time difference $\Delta\mathrm{t}$ is computed from a correlation function. Thus, the spatial and temporal variability of the WTC field is taken into account by the correlation function. In the absence of the knowledge of an empirical covariance model of the background field, the correlation function $\mathrm{F}(r,\Delta\mathrm{t})$ can take the form of a product of two stationary Gaussian decays (Schüler, 2001; Leeuwenburgh, 2000), i.e.,

$$\mathrm{F}(r, \Delta\mathrm{t}) = \mathrm{F}_r(r) \times \mathrm{F}_{\Delta\mathrm{t}}(\Delta\mathrm{t}) = e^{-\frac{r^2}{D}} \times e^{-\frac{\Delta\mathrm{t}^2}{T}} \tag{10}$$

where r is the distance and $\Delta\mathrm{t}$ is the time interval between acquisitions of each pair of points, and D and T are the spatial and temporal correlation scales, respectively.

In summary, the implementation of the method requires the knowledge of the following quantities:

- First guess of *WTC*
- Variance of the *WTC* field
- White noise associated with the measurements of each *WTC* data set (required to compute the diagonal elements of the variance-covariance matrix, A_{ik})

- Parameters defining the correlation function: space and time correlation scales.
- Space and time search radius

3.2 Development choices and Trade-offs

OA implementation

Concerning the OA implementation, the adopted parameters are described below. For the first guess a weighted average of all selected *WTC* values within the space and time search radii was adopted, the weights computed from the set of observations according to Bretherton et al. (1976).

The variance of the *WTC* field was determined from a two years dataset of the ECMWF operational model at 0.25°×0.25° and 6 hours intervals, already performed in the scope the work presented in Fernandes et al. (2010).

For the white noise associated to each data type the following values were adopted: GNSS: 0.5 cm (Fernandes et al., 2010); SI-MWR: from 0.81 to1.22 cm, depending on sensor, see Table 1 (Fernandes et al., 2013b); ECMWF operational model: 1.5 cm. The value of the error adopted for the ECMWF-model-derived *WTC*, which is known to be larger than the former two, was chosen to reduce the influence of the model in the computation and to balance the weight between the various types of observations.

Table 1. White noise associated to each SI-MWR sensor (RMS of the differences between the *WTC* from each sensor and AMR, after calibration with respect to AMR).

Satellite	Sensor	White noise (cm)
AQUA	AMSR-E	0.81
Coriolis	WindSat	0.89
DMSP-F15	SSM/I	1.02
DMSP-F16	SSM/IS	0.96
DMSP-F17	SSM/IS	1.02
MetOp-A	AMSU-A	1.13
NOAA-15	AMSU-A	1,22
NOAA-16	AMSU-A	1.13
NOAA-17	AMSU-A	1.20
NOAA-18	AMSU-A	1.18
NOAA-19	AMSU-A	1.17
TRMM	TMI	1.09

The space correlation scales were determined from a set of ECMWF operational model grids at 0.125°×0.125°, well distributed over the year 2013. The computations were performed for a grid of points centered on 2°× 2° "boxes". For each of these central points, analyses were made on boxes of 2°× $\Delta\lambda$°, where $\Delta\lambda$ = min (2°/ cos φ, 2°), where φ and λ stand for latitude and longitude, respectively. This warrants that all analyses are made on boxes of approximately the same size. For each box, the

correlation between all pairs of points separated by a distance R, for classes of R spaced by 10 km, were determined. The set (R, corr(R)) forms the correlation table for each box. The corresponding correlation scale D is obtained by either fitting a Gaussian function to the correlation table or by computing the value of R corresponding to a correlation equal to 1/*e*. Both approaches give similar results and the resulting spatial correlation scales are within 40 to 93 km (Figure 1).

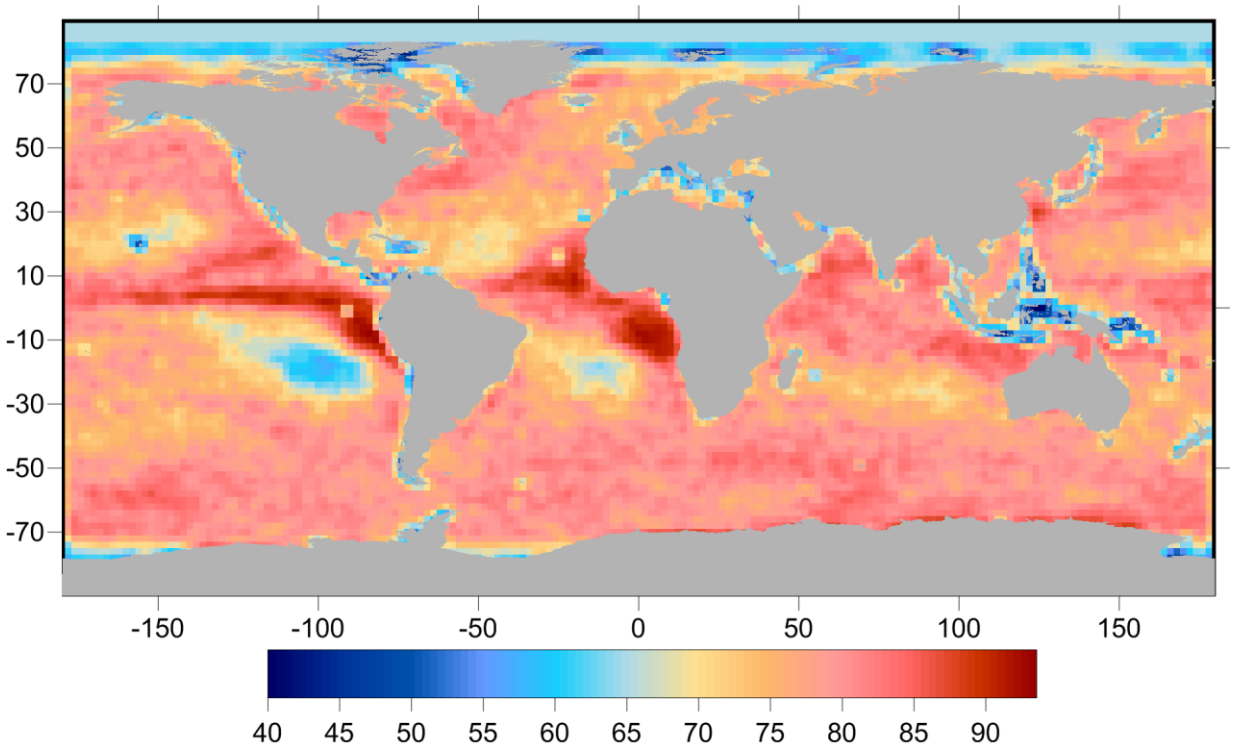

Figure 1 – Spatial correlation scales (in km) for the *WTC* as determined from a set of ECMWF Operational Model grids at 0.125°×0.125° well distributed over the year 2013.

For the temporal correlation scales, in the absence of time to perform a similar analysis within the time frame of this project, the value of 100 minutes quoted by Bosser et al. (2007) was adopted.

The data used for each WTC estimation are the WTC values from the independent data sets within the spatial and temporal influence regions, centered at the location and instant of the altimeter measurement at which the estimation is required. These values should be close to the spatial and temporal correlation scales. In practice, a search radius of 100 km was adopted for all data types. For the temporal search radius, values of 100, 110 and 180 minutes were adopted for GNSS, SI-MWR and ECMWF, respectively. The second value aims at ensuring that SI-MWR data from two adjacent satellite tracks can be used (separated in time by 100-105 minutes) and the third value aims at allowing the use of data from at least one ECMWF grid (consecutive grids are separated by 6 h).

To reduce the computation time, a maximum number of 25 GNSS and 25 SI-MWR measurements were used, those with the largest weights, according to their distance and time difference with respect to the point of estimation. Concerning ECMWF data values, the four points closest to the estimation point were used. The continuous use of ECMWF measurements, although with a lower weight than all

other data types, reduces the discontinuities of the correction in the transition zones defined by the availability of SI-MWR or GNSS data.

Input data sets

As mentioned above, wet path delays from the following three data types are used: SI-MWR, GNSS and ECMWF operational model.

The SI-MWR data set is composed of data from 11 different sensors, previously calibrated with respect to AMR, as previously reported in the "CP4O Progress Report on the Improvement of the Wet Tropospheric Correction for the CryoSat-2 mission" and also in Fernandes et al. (2013b).

Data from 11 missions are available for the computation period (January 2012 to January 2013): 6 AMSU–A on-board MetOp-A, NOAA-15, NOAA-16, NOAA-17, NOAA-18, NOAA-19; 3 SSM/I and SSM/IS on-board F15, F16, F17; WindSat on-board Coriolis, and TMI on board TRMM (see Tables 2 and 3, also from Fernandes et al. (2013b)). These SI-MWR provide images which allow the spatial coverage of 70-100% of CS-2 data if a temporal search radius of 110 minutes is allowed.

The spatial coverage of the various datasets for CS-2 sub-cycles 31 and 35 is shown in Figure 2 and Figure 3, respectively.

Table 2. Main characteristics of the sensors with scanning MWR images of TCWV available for this study (plus AMSR-E). The scale factor of product is the value required to multiply the original product value to get the TCWV in mm. All products are swath except the last two, which are grid products. (*) Swath product from NOAA CLASS database; (**) Grid product from Remote Sensing Systems (RSS). (***) Value provided is the central pixel size (maximum pixel size is 130 km).

Sensor	Pixel size (km)	Swath width (km)	Number of (lines, pixels)	Name of product	Scale factor of product	Channels used to retrieve TCWV (GHz)
AMSR-E	9 km	1625	(variable,243)	Med_res_vapor	0.01	18.7/23.8/36.5
AMSU-A	50 km (***)	2200	(variable,30)	TPW	0.1	23.8/31.4
TMI	10 km	878	(variable,104)	Columnar_water_vapor	0.01	19.35/21.3/37.0
SSM/I (*)	25 km	1420	(variable,64)	TPW	0.1	19.35/22.235/37.0
SSM/I, SSM/IS (**)	0.25°	1790 -1850	(720,1440)	VAPOR	0.3	19.35/22.235/37.0
WindSat	0.25°	1400	(720,1440)	VAPOR	0.3	18.7/23.8/37.0

Table 3. Main orbital characteristics (compared with those of CryoSat-2) of the satellites with scanning MWR images of TCWV available for this study (plus Aqua/AMSR-E). Grey-shaded lines refer to gridded products and the remaining to swath products. LTAN is the Local Time of the Ascending Node. (*) RSS products, corrected for RADCAL beacon interference are used. (**) Available only up to April 2013.

Satellite	Sensor	height (km)	inclination (º)	period (min)	Sun-synch. orbit	LTAN Jan 2011 (hh:mm)	LTAN Jan 2012 (hh:mm)	data availability for CryoSat-2
CryoSat-2	-	717	92.0	93.2	No	N/A	N/A	since April 2010
Aqua	AMSR-E	705	98.0	99.0	Yes	13:36	-	until Oct 2011
NOAA-19	AMSU-A	870	98.7	102.1	Yes	13:32	13:32	until present
NOAA-18	AMSU-A	854	98.7	102.1	Yes	14:07	14:30	until present
DMSP-F15	SSM/I	850	98.8	102.0	Yes	16:44	16:05	(*)
NOAA-15	AMSU-A	807	98.5	101.1	Yes	16:35	16:35	until present
Coriolis	WindSat	830	98.8	101.6	Yes	17:54	17:54	until present
DMSP-F17	SSM/IS	850	98.8	102.0	Yes	17:30	18:06	until present
DMSP-F16	SSM/IS	845	98.9	101.8	Yes	19:12	18:30	until present
NOAA-17	AMSU-A	810	98.7	101.2	Yes	20:20	19:40	(**)
NOAA-16	AMSU-A	849	99.0	102.1	Yes	19:16	20:00	until present
MetOp-A	AMSU-A	817	98.7	101.4	Yes	21:26	21:27	until present
TRMM	TMI	402	35.0	93.0	No	N/A	N/A	until present

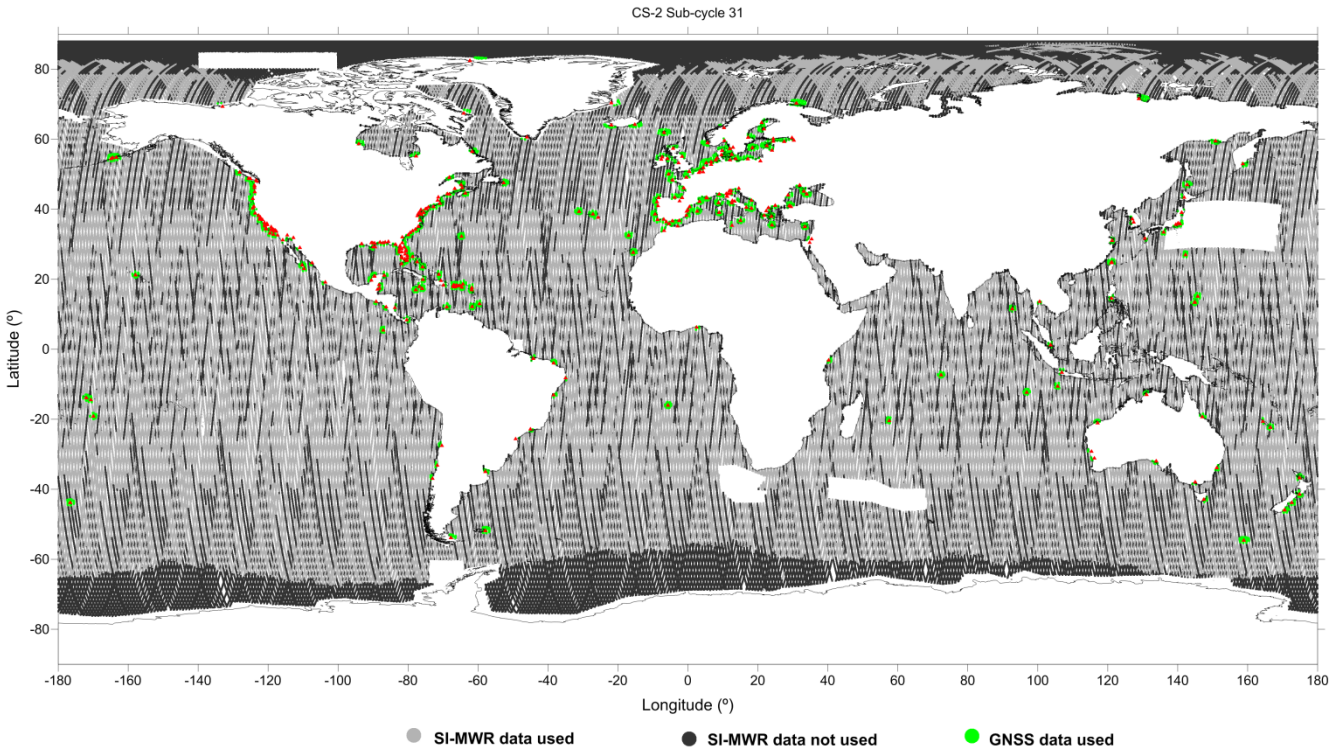

Figure 2 – Spatial coverage of the various datasets for CS-2 sub-cycle 31. Red triangles represent the location of the GNSS stations.

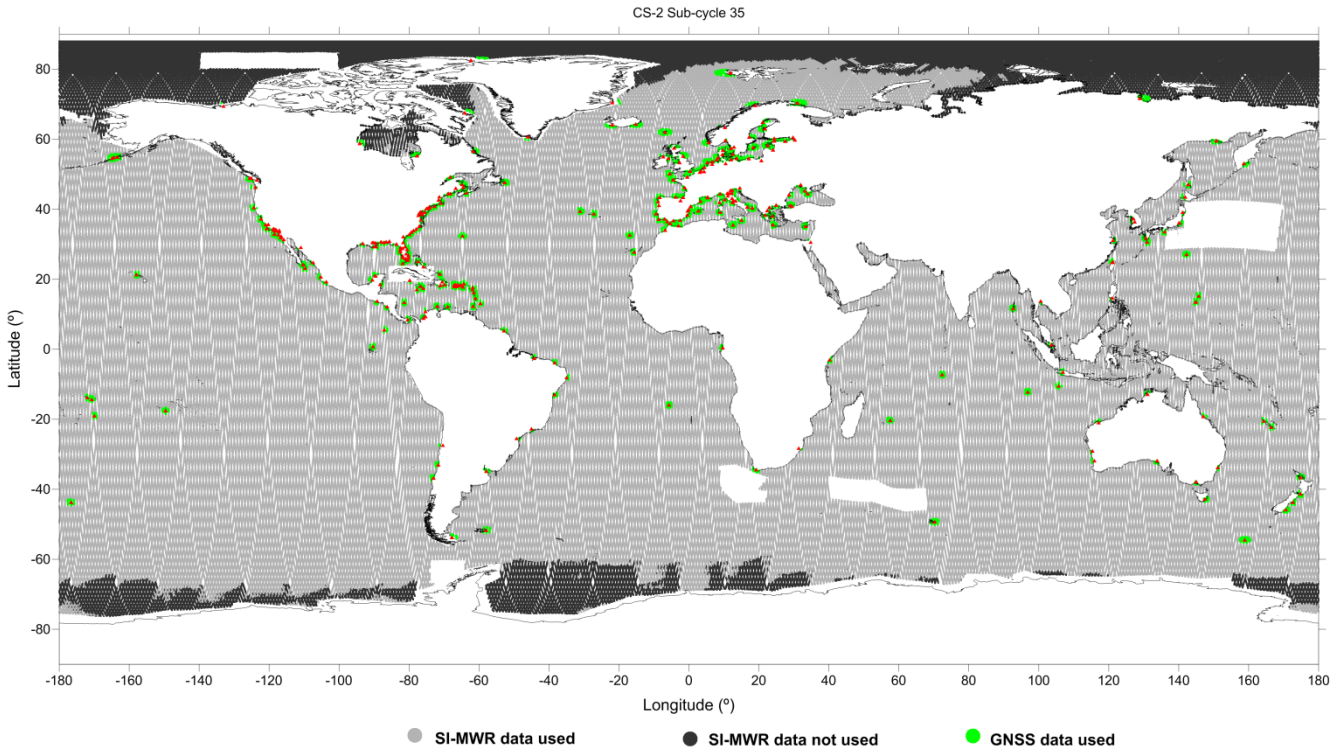

Figure 3 – Spatial coverage of the various datasets for CS-2 sub-cycle 35. Red triangles represent the location of the GNSS stations.

Concerning GNSS, data from an average number of 400 stations are available for each day. The number of stations with available online zenith total delays (ZTD) is continuously increasing as shown in Figure 4. The location of the whole set of coastal GNSS stations used in this study is shown in Figure 5.

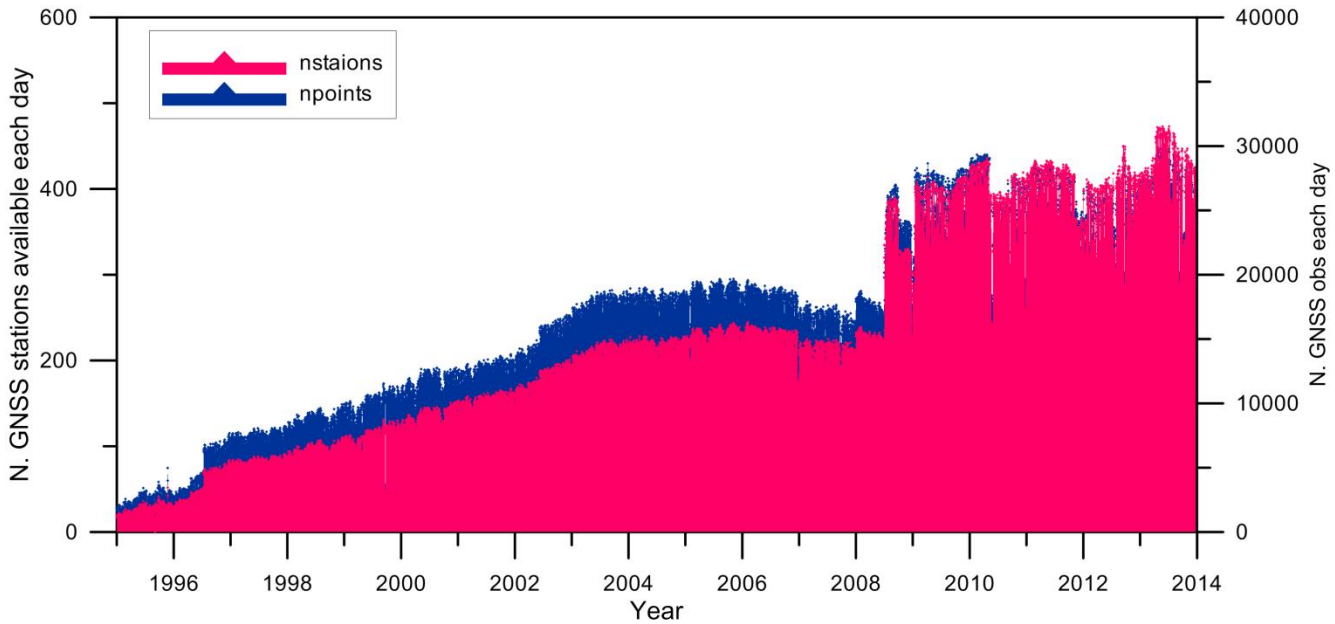

Figure 4 – Number of GNSS stations and observations per day, since 1995.

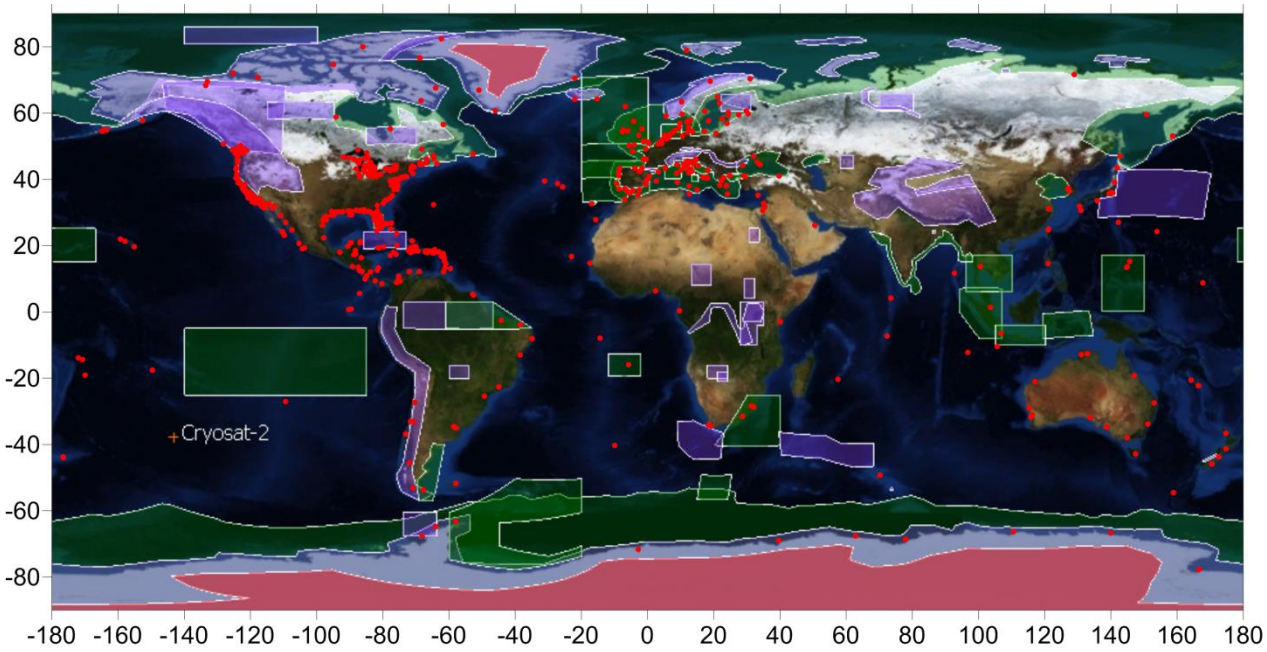

Figure 5 – Location of the whole set of coastal GNSS stations overlaid on CS-2 mode mask 3.4.

Concerning the NWM, it was found that for the period of CS-2 mission, the best available model is the ECMWF operational model. It is known that the ECMWF operational model does not provide a consistent climatological data record, as its several updates resulted in a number of discontinuities over time. Therefore, and in spite of its better spatial resolution, for long-term studies involving the period prior to 2004 ERA Interim is a better option. However, for the period of CS-2 the use of ECMWF operational model for the computation of the wet tropospheric correction provides better results than ERA Interim, particularly due to its finer spatial resolution. This is illustrated in figures 6 to 9 which show the increase in SLA variance for CS-2 and J2 data obtained with ERA Interim when compared to ECMWF operational model. Since a consistent bias of ~5 mm was found between the WTC derived from ECMWF operational model and that of AMR for the whole period of the CS-2 mission, prior to their use in the OA, a constant value of 5mm was added to the ECMWF WTC-derived values.

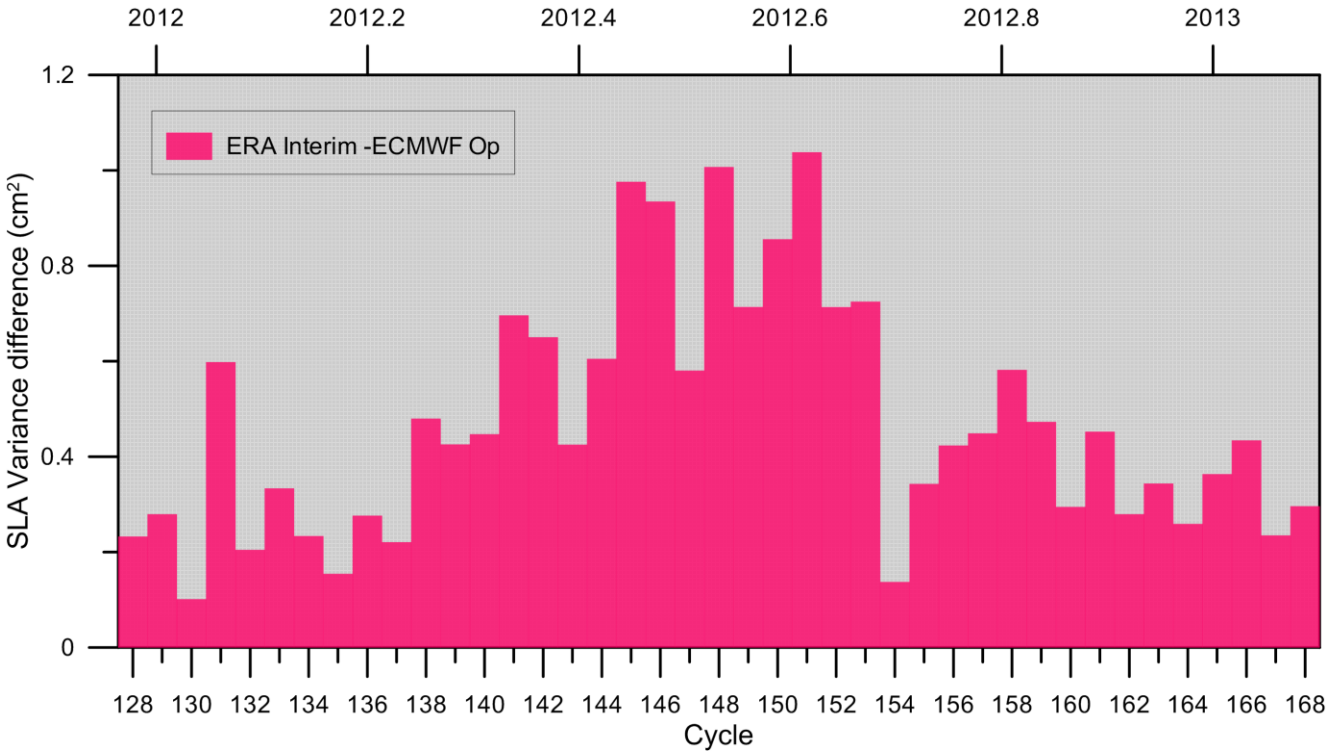

Figure 6 – SLA variance differences (cm^2), for each J2 cycle, between ERA Interim and ECMWF Operational models.

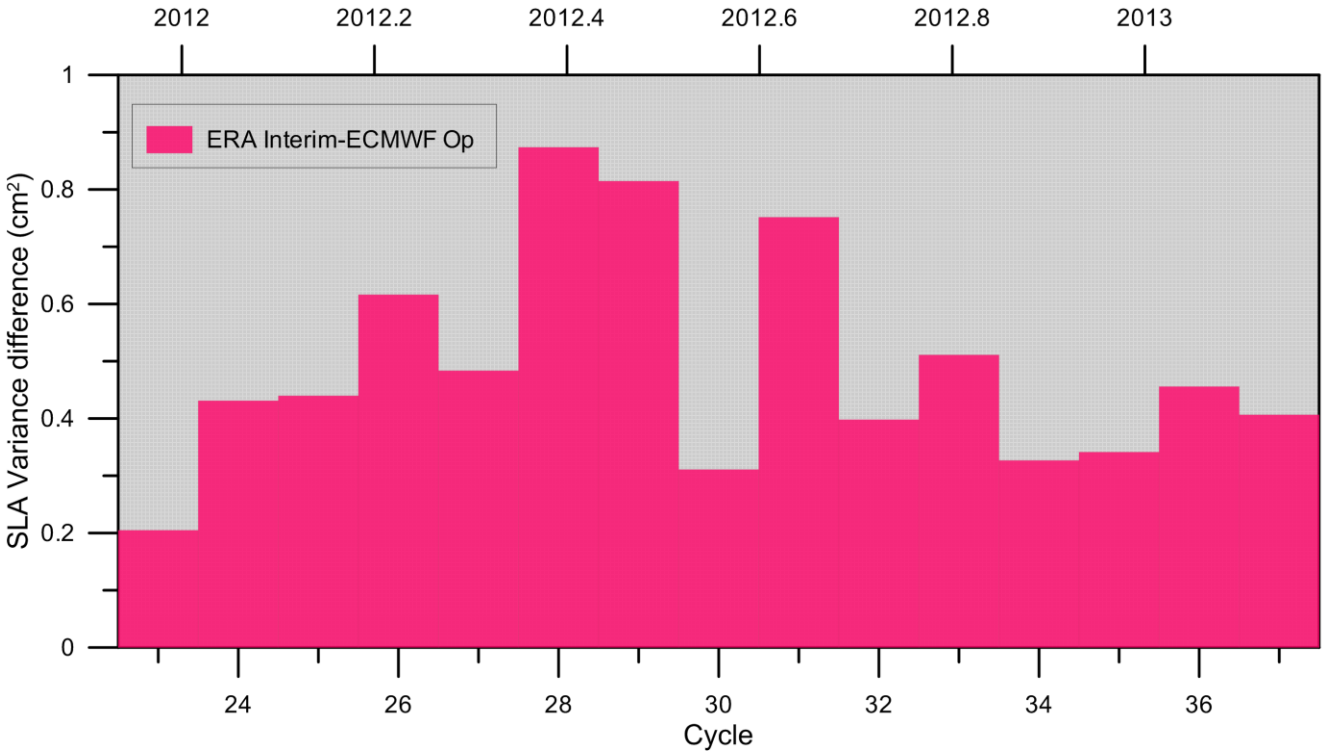

Figure 7 – SLA variance differences (cm^2), for each CS-2 sub-cycle, between ERA Interim and ECMWF Operational models.

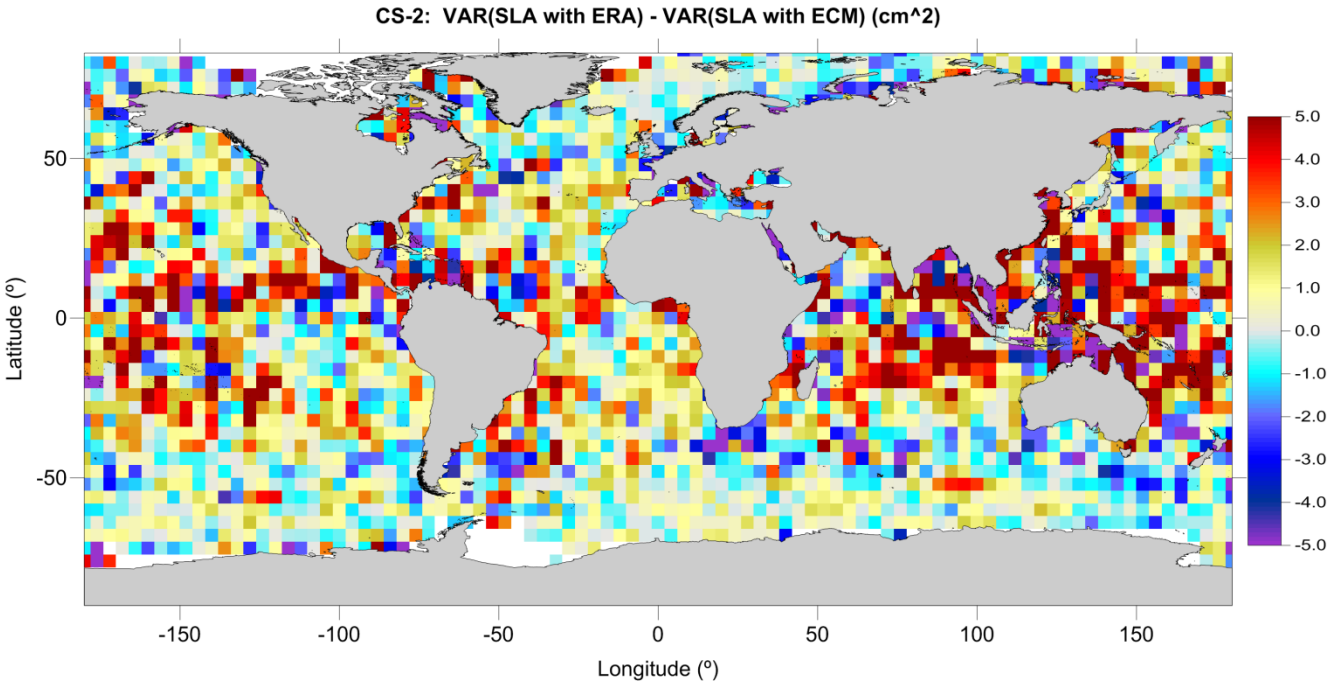

Figure 8 – SLA variance difference at CS-2 crossovers (cm^2) between ERA Interim and ECMWF operational models.

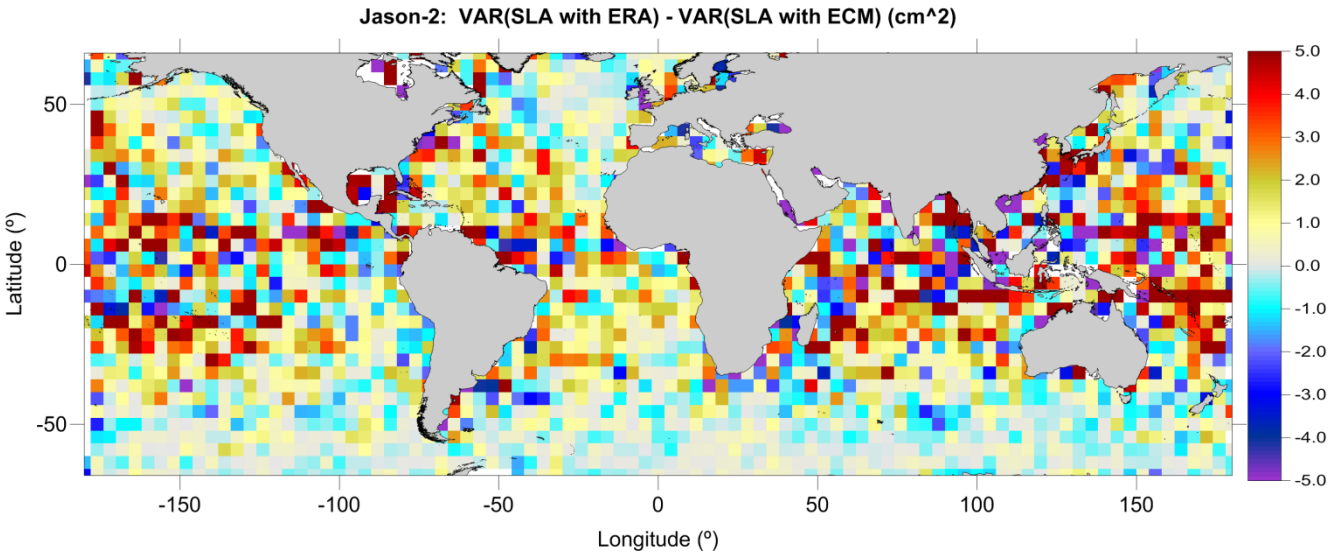

Figure 9 – SLA variance difference at J2 crossovers (cm^2) between ERA Interim and ECMWF operational models.

3.2.1 Scientific results

The DComb algorithm has been implemented globally and applied both to J2 and CS-2 for the period for about 13 months, from January 2012 to January 2013. Applying the algorithm also to J2 allows a comparison of the correction to that directly derived from the AMR on J2 (note that no measurements from AMR are used in DComb for the computation of the WTC for J2).

For practical reasons the data used in most of the study were J2 and CS-2 data from the Radar Altimeter Database System (RADS). In addition, the correction was also computed for the months of July 2012 and January 2013 for data files provided by ESA. The latter dataset was provided to CLS for use in the independent validation task performed in WP5000.

Figure 10 illustrates the results for J2 cycle 127, pass 222. The striking feature of this figure is how well the DComb WTC captures the signal present in AMR at latitude 40ºN, which is not present in the ECMWF model. Figure 11 illustrates the WTC for CS-2 sub-cycle 35.

The product validation report (PVR) presents the results and validation of the products computed from the RADS dataset. The results obtained for the ESA dataset are presented by CLS in separate deliverables in the scope of WP5000.

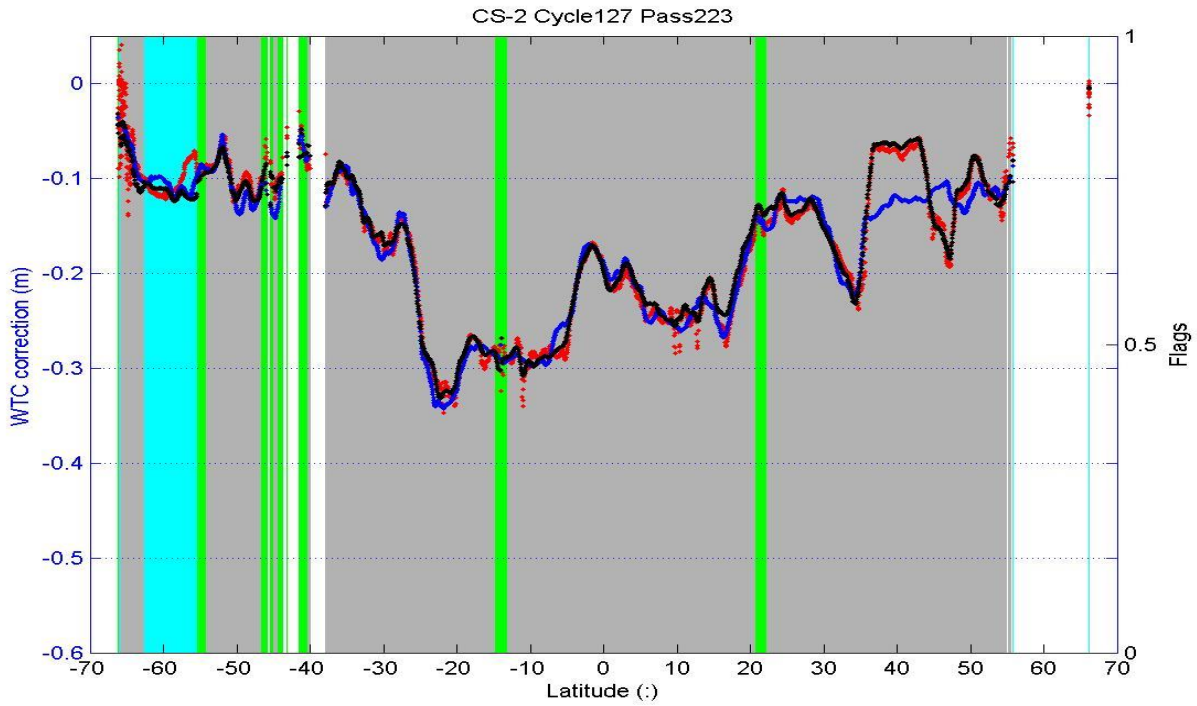

Figure 10 – Various WTC for J2 cycle 127 pass 223: ECMWF model (blue), AMR (red) and DComb (black). The shaded areas represent regions for which SI-MWR observations (grey), GNSS (green) or model only (blue) are available.

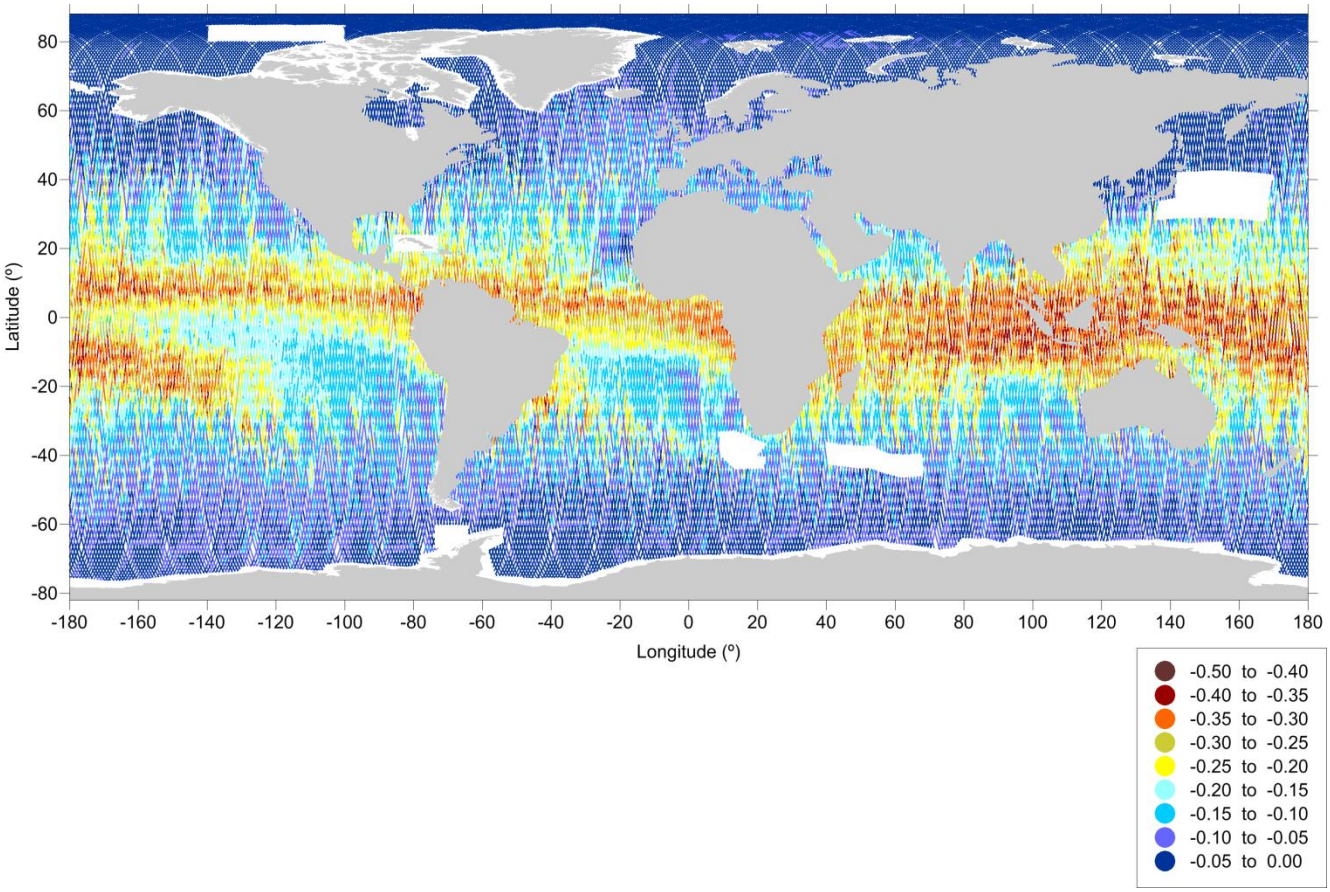

Figure 11 – DComb WTC (in m) for CS-2 sub-cycle 35.

3.2.2 Error analysis

As described above, besides the estimation of the WTC, the OA also provides the associated formal error. The error is function of the signal variance of the field and of space and time distribution of the observations. Since the coverage is not uniform for all sub-cycles, the errors will also vary with this coverage. This is illustrated in Figures 12 and 13 for sub-cycles 31 and 35, respectively.

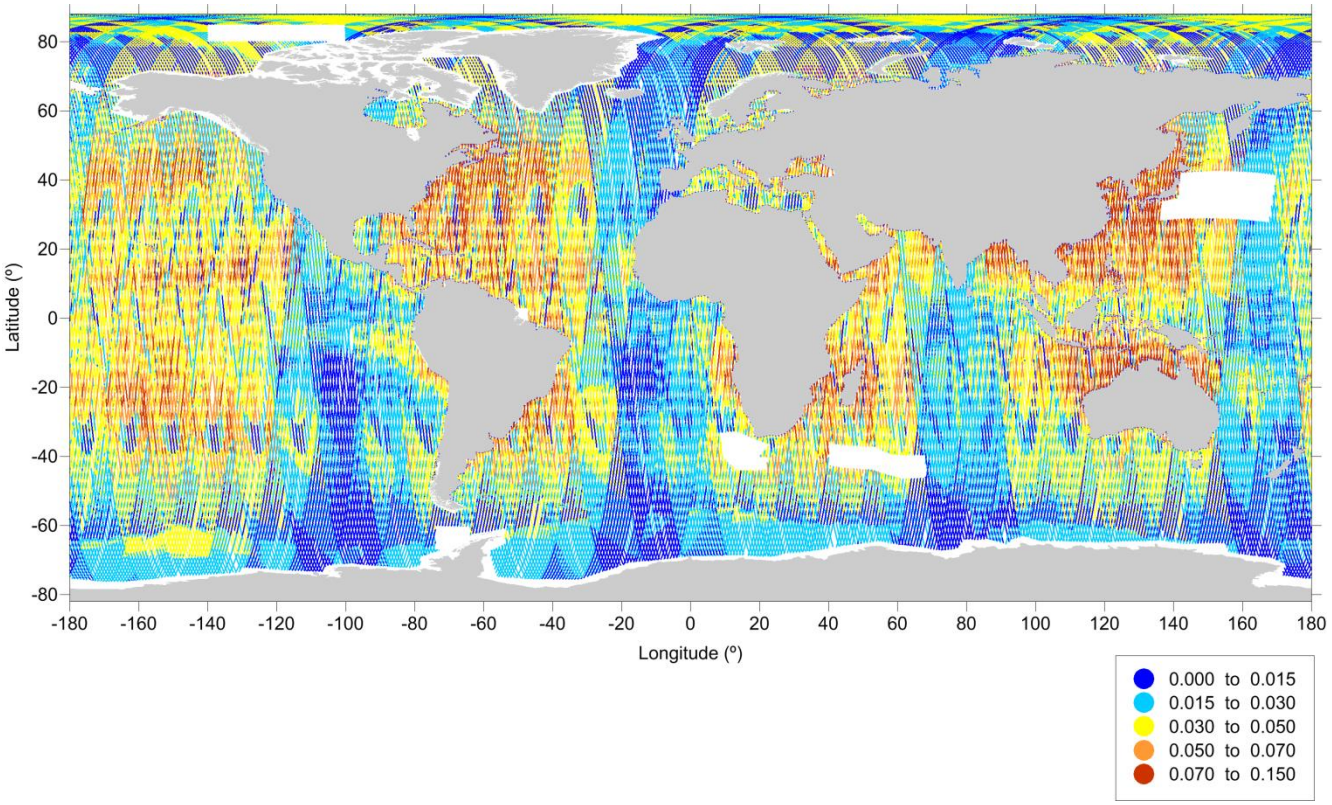

Figure 12 – Formal error (in m) for CS-2 sub-cycle 31.

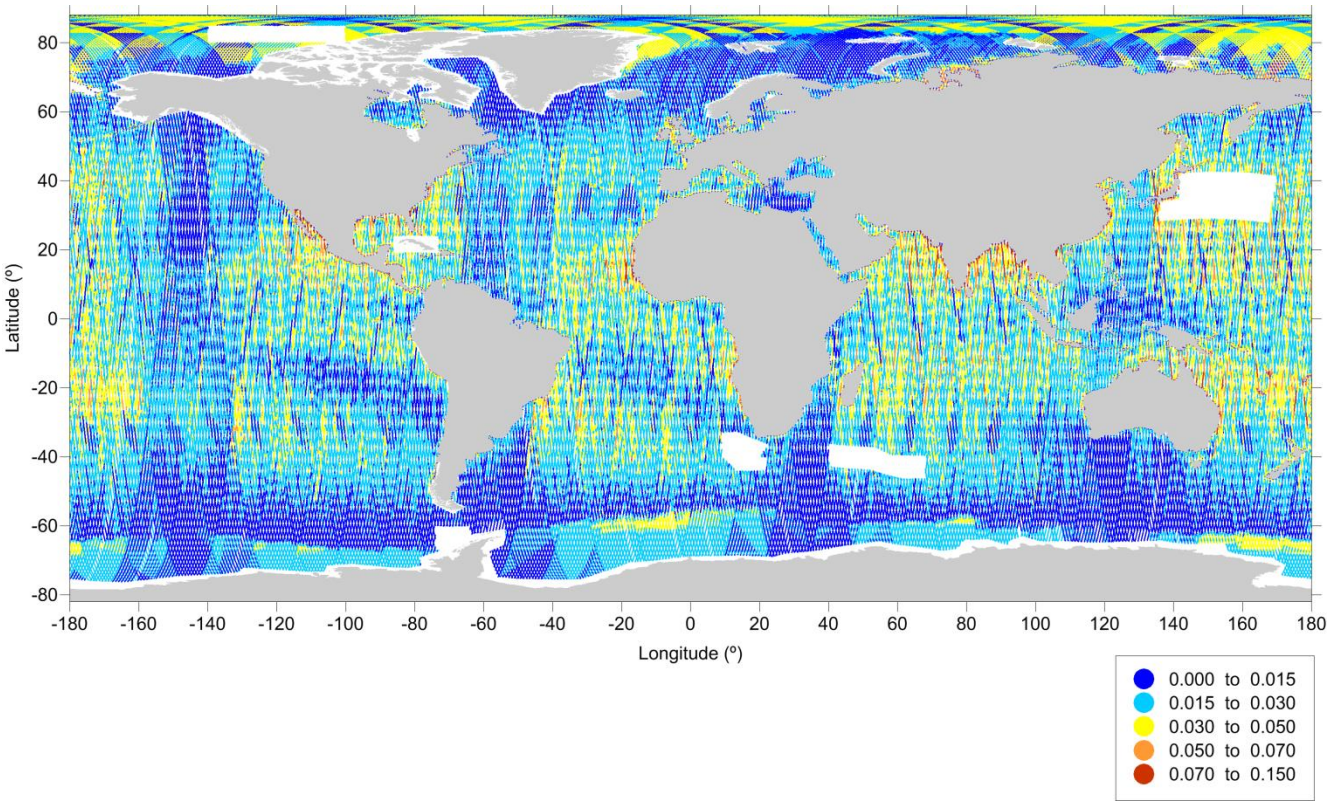

Figure13 – Formal error (in m) for CS-2 sub-cycle 35.

4. Assumptions, Constraints, and Limitations

4.1 Practical Considerations

4.1.1 Input data

A mandatory task that had to be performed in advance was the analysis and inter-calibration of all datasets for the computation of the wet path delay of altimeter measurements over open ocean, polar regions, and coastal zones, for their use in the DComb algorithm. In this context, the dataset of total column water vapour (TCWV) images acquired by the various SI-MWR on board RS missions is of particular relevance due to data amount and coverage (both in space and time) and the variety of instruments acquiring such data, which did thus require proper inter-calibration.

The main limitation on the use of SI-MWR data is the fact that they are not collocated in time and space to the altimeter measurement, thus leading to a lower accuracy when compared to WTC derived from the on-board MWR. In addition, as shown in the "CP4O Progress Report on the Improvement of the Wet Tropospheric Correction for the CryoSat-2 mission" and on Fernandes et al. (2013b), the data coverage is not uniform, leading to time variable accuracy. In spite of that, for periods of good data coverage the results are remarkable and the overall improvement with respect to ECMWF operational model is evident.

The GNSS-derived WTC has been subject to thorough analyses by the authors in the scope of previous studies, mostly within other ESA-funded projects (COASTALT and Sea Level CCI - Phase 1), and a brief description of the main conclusions has been provided in D2.1 – Preliminary Analysis Report.

Concerning the use of GNSS data to compute the WTC, the main limitation is the sparseness of the GNSS stations. In spite of that, where available this is a very valuable dataset with clear impact in the coastal regions, of major importance for CS-2.

4.1.2 Ancillary information

For practical reasons the data used in most of the study were J2 and CS-2 data from the Radar Altimeter Database System (RADS). For this dataset the correction was computed and validated for the period of about 13 months, from January 2012 to January 2013.

In addition, the correction was also computed for the periods of July 2012 and January 2013 for data files provided by ESA. The latter dataset, which unlike that retrieved from RADS contains data for all CS-2 acquisition modes, was provided to CLS for use in the independent validation task performed in WP5000 – Impact Assessment.

More information on these datasets is given in D4.2 – Product Validation Report.

4.1.3. Output

Two sets of files are provided as an output for use in WP5000 – Impact Assessment. Each set contains the *WTC* for CS-2 sub-cycles 29 and 30 (July 2012) and sub-cycles 36 and 37 (January 2013).
Dataset 1 – Computed for CryoSat-2 data points available in RADS. This includes all ocean points (Surface type=0) and the land points closest to the coast, up to a distance from coast of 50 km. This includes all LRM data and most of SAR mode data.
Dataset 2 – Computed for files provided by ESA, containing points for all surface types and all instrument modes.

All fields contained in Dataset 1, except for those related with the DComb WTC, were extracted from RADS.

The ESA files contained only time, latitude, longitude, surface type and instrument mode. These files had to be processed using the following steps:

- The sub-cycle and pass numbers according to RADS convention were introduced, which are required to run the DComb algorithm;
- Duplicated points were removed;
- Only 1-Hz points were extracted (those for which the surface type and instrument mode were defined);
- The WTC from ECMWF operational model grids at 0.125°×0.125° spacing and 6 h time interval was interpolated for the time and location of each measurement.

All files are provided at 1-Hz.

Two WTC data sets were generated because the RADS data are easier to handle and so were selected for the global scale validation, whilst a second dataset was needed for the specific coverage of the ESA dataset provided for the independent assessment by CLS. The coverage and precise time / location of data points differ between the RADS and ESA CS-2 altimeter datasets, so the same data could not be used for both evaluations. Regarding the points for the LRM and SAR modes, the two datasets contain approximately the same points, although with different time and locations. The ESA dataset contains points for a few SAR mode regions which are not present in RADS, but there is also a very small number of track portions present in RADS which are not present in the ESA files.

The time interval between consecutive points in the ESA files is not constant. It can vary from 0.88 s to 0.94 s, while in RADS the time interval is always ~0.94 s. To match the two data sets the time difference between TAI and UTC must be accounted for. Due to the fact that the time interval between the 1-Hz measurements is not the same, for a given epoch, the location of the corresponding points must be computed by interpolation. For a WTC comparison the closest point in time can be used, provided that the time difference between the matching points is small enough, e.g. < 0.60 s.

The DComb WTC has been computed only for ocean points, therefore only these points should be used in the comparisons.
The correction is provided in NetCDF files with the fields listed below.

List of provided fields

Cycle	Sub-cycle number according to RADS convention
Pass	Pass number according to RADS convention
Tisec	Time in seconds since 2000-01-01 00:00:00 (UTC) – on Dataset 1
Tisec	Time in seconds since 2000-01-01 00:00:00 (TAI) – on Dataset 2, as in original ESA files
MJD	Modified Julian date (UTC)
Latitude	Latitude (degrees north)
Longitude	Longitude (degrees east)
wet_ECMWF	WTC from the ECMWF operational model (metres)
wet_DComb	WTC from the DComb algorithm (metres)
formal_error	Formal error of the wet_DComb estimate (metres)
Surface_type	0=open ocean, 1=enclosed seas and lakes, 2=continental ice, 3=land
N_obs	Total number of observations used
flag_GNSS	1 if GNSS observations were used
flag_ECMWF	1 if ECMWF operational model was used
flag_SI-MWR	1 if SI-MWR observations were used

The information given above is also repeated in D4.2

4.2 Programming considerations

Due to the large amount of data to be handled various strategies needed to be implemented to speed up the computations. For example, the number of GNSS and SI-MWR observations is limited to 25 in both cases.

4.3. Quality control

During the various steps of the computations (e.g., preparation of input data, output control) statistical and graphical analysis are performed in order to detect outliers, ice and land contamination, discontinuities, etc..

4.4. Exception handling

Not applicable.

5. References

Bevis, M., S. Businger, S. Chiswell, T. A. Herring, R. A. Anthes, C. Rocken, and R. H. Ware (1994), GPS Meteorology - Mapping Zenith Wet Delays onto Precipitable Water, *Journal of Applied Meteorology*, *33*(3), 379-386, doi:10.1175/1520-0450(1994)033

Bosser P., O. Bock, J. Pelon, and C. Thom, "An improved mean-gravity model for GPS hydrostatic delay calibration," IEEE Geosci. Remote Sens. Lett., vol. 4, no. 1, pp. 3–7, Jan. 2007.

Bretherton F. P., R. E. Davis, and C. B. Fandry, "A technique for objective analysis and design of oceanographic experiment applied to MODE-73," Deep-Sea Res., vol. 23, pp. 559–582, 1976.

Dee, D. P., et al. (2011), The ERA-Interim reanalysis: configuration and performance of the data assimilation system, *Quarterly Journal of the Royal Meteorological Society*, *137*(656), 553-597, doi:10.1002/qj.828.

Fernandes, M. J., C. Lazaro, A. L. Nunes, N. Pires, L. Bastos, and V. B. Mendes (2010), GNSS-Derived Path Delay: An Approach to Compute the Wet Tropospheric Correction for Coastal Altimetry, *Ieee Geoscience and Remote Sensing Letters*, *7*(3), 596-600, doi:10.1109/lgrs.2010.2042425.

Fernandes, M. J., N. Pires, C. Lázaro, and A. L. Nunes (2013a), Tropospheric Delays from GNSS for Application in Coastal Altimetry, *Advances in Space Research*, *51*(8), doi:10.1016/j.asr.2012.04.025.

Fernandes, M.J., A.L. Nunes, C. Lázaro (2013b) Analysis and Inter-Calibration of Wet Path Delay Datasets to Compute the Wet Tropospheric Correction for CryoSat-2 over Ocean. Remote Sens. 2013, 5, 4977-5005.

Fernandes, M.J.; Lázaro, C.; Nunes, A.L.; Scharroo, R. (2014), Atmospheric Corrections for Altimetry Studies over Inland Water. Remote Sens. 2014, 6, 4952-4997.

Keihm, S. J., M. A. Janssen, and C. S. Ruf (1995), TOPEX/POSEIDON MICROWAVE RADIOMETER (TMR) .3. WET TROPOSPHERE RANGE CORRECTION ALGORITHM AND PRE-LAUNCH ERROR BUDGET, *IEEE Trans. Geosci. Remote Sensing*, *33*(1), 147-161, doi:10.1109/36.368213.

Keihm, S. J., V. Zlotnicki, and C. S. Ruf (2000), TOPEX Microwave Radiometer performance evaluation, 1992-1998, *IEEE Trans. Geosci. Remote Sensing*, *38*(3), 1379-1386, doi:10.1109/36.843032.

Kouba, J. (2008), Implementation and testing of the gridded Vienna Mapping Function 1 (VMF1). *J. Geodesy*, 82, 193–205. doi: 10.1007/s00190-007-0170-0

Leeuwenburgh O., "Covariance modelling for merging of multisensor ocean surface data," in Methods and Applications of Inversion. New York: Springer-Verlag, 2000.

Mendes, V.B. (1999) Modeling the Neutral-Atmosphere Propagation Delay in Radiometric Space Techniques. Ph.D. Dissertation, Department of Geodesy and Geomatics Engineering, University of New Brunswick, Fredericton, NB, Canada, 1999.

Mendes, V.B.; Prates, G.; Santos, L.; Langley, R.B. (2000), An Evaluation of the Accuracy of Models of the Determination of the Weighted Mean Temperature of the Atmosphere, In Proceedings of ION 2000 National Technical Meeting, Anaheim, CA, USA, 26–28 January 2000.

Miller, M., R. Buizza, J. Haseler, M. Hortal, P. Janssen, and A. Untch (2010), Increased resolution in the ECMWF deterministic and ensemble prediction systems., *ECMWF Newsletter*, *124*, 10-16.

Schüler J., "On ground-based GPS tropospheric delay estimation," Ph.D. dissertation, Universität der Bundeswehr, München, Germany, 2001.

Stum, J., P. Sicard, L. Carrere, and J. Lambin (2011), Using Objective Analysis of Scanning Radiometer Measurements to Compute the Water Vapor Path Delay for Altimetry, *IEEE Trans. Geosci. Remote Sensing*, *49*(9), 3211-3224, doi:10.1109/tgrs.2011.2104967.

6. Abbreviations and Acronyms

AMR	Advanced Microwave Radiometer (AMR)
AMSR-E	Advanced Microwave Scanning Radiometer-Earth Observing System
AMSU-A	Advanced Microwave Sounding Unit A
ATBD	Algorithm Theoretical Basis Document
CS-2	CryoSat-2
DComb	Data Combination (algorithm)
DMSP	Defense Meteorological Satellite Program
ECMWF	European Centre for Medium-Range Weather Forecasts
EPN	EUREF Permanent Network
ERA	ECMWF ReAnalysis
ESA	European Space Agency
EUMETSAT	European Organisation for the Exploitation of Meteorological Satellites
GDR	Geophysical Data Records
GNSS	Global Navigation Satellite Systems
GPD	GNSS-derived path delay (algorithm)
J1	Jason-1
J2	Jason-2
MWR	microwave radiometers
NASA	National Aeronautics Space Administration
NOAA	National Oceanic and Atmospheric Administration
NRL	Naval Research Laboratory (NRL)
NWM	numerical weather models
OA	Objective Analysis
PW	Precipitable Water
RADS	Radar Altimeter Database System
RA-MWR	MWR onboard altimetric missions
RS	Remote Sensing
SAR	Synthetic Aperture Radar
SI-MWR	Scanning Imager MWR
SLA	Sea Level Anomaly
SSM/IS	Special Sensor Microwave Imager/Sounder
TCWV	Total Column Water Vapour
TMI	TRMM Microwave Imager
T/P	TOPEX/Poseidon
TRMM	Tropical Rain Measuring Mission (TRMM)
U.Porto	University of Porto
WTC	Wet Tropospheric Correction
ZWD	Zenith Wet Delay

7. Acknowledgements

The authors would like to thank the European Centre for Medium-Range Weather Forecasts (ECMWF) for making available the ERA Interim data on the ECMWF data server, and all organizations which provide the water vapour products used in this study: NOAA through its Comprehensive Large Array-Data Stewardship System (CLASS), Remote Sensing Systems, the Global Hydrology Resource Center and the National Snow and Ice Data Center.